

Engineering Notes

ENGINEERING NOTES are short manuscripts describing new developments or important results of a preliminary nature. These Notes should not exceed 2500 words (where a figure or table counts as 200 words). Following informal review by the Editors, they may be published within a few months of the date of receipt. Style requirements are the same as for regular contributions (see inside back cover).

Simple Experimental Method to Estimate the Lift of Airfoils

Lance W. Traub*

Embry-Riddle Aeronautical University,
Prescott, Arizona 86301

DOI: 10.2514/1.36132

Nomenclature

a, b	=	constants
C_l	=	lift coefficient
c	=	airfoil chord
H	=	distance from the bound vortex to the tunnel wall
h	=	distance from the bound vortex to the pitot-static tube
l	=	distance from the pitot-static tube to the tunnel wall, lift
U_∞	=	freestream velocity
V	=	velocity measured by the pitot-static tube
\bar{V}	=	corrected measured velocity accounting for influence of image vortices
w_v	=	bound-vortex-induced velocity
Γ	=	circulation
ρ	=	density

Subscripts

l	=	lower
u	=	upper

Introduction

THE measurement of airfoil lift is among the most fundamental characterizations in the evaluation of a profile's performance. Historically, sectional lift performance is measured using a force balance, airfoil pressure integration, or wall pressure integration. These methods, although well-established and verified, have potential limitations, depending on the test requirements and conditions. Force balances, if external, are intrusive. They need to be accurately calibrated, incur tare and interference [1], and if used for 2-D testing, may have clearance issues between the tunnel wall and wing end. For low Reynolds number testing, balance design can be challenging due to the very small loads. If an internal sting balance is used, it requires calibration and may not function well with the small load magnitudes. The sting may affect the flow in its vicinity. Pressure integration increases the complexity of the model design significantly and may be complicated by leaking and blocked ports.

Received 10 December 2007; revision received 10 January 2008; accepted for publication 10 January 2008. Copyright © 2008 by Lance W. Traub. Published by the American Institute of Aeronautics and Astronautics, Inc., with permission. Copies of this paper may be made for personal or internal use, on condition that the copier pay the \$10.00 per-copy fee to the Copyright Clearance Center, Inc., 222 Rosewood Drive, Danvers, MA 01923; include the code 0021-8669/08 \$10.00 in correspondence with the CCC.

*Associate Professor, Aerospace Engineering Department. Member AIAA.

Additionally, tapings can cause premature boundary-layer transition [2]. Locating ports near the trailing edge can be challenging in smaller-scale models. At low Reynolds numbers, resolution and accuracy of the pressure measurement system can be an issue. Wall-signature pressure integration,[†] although not widely used, does suffer from potential boundary-layer effects (localized separation) altering port pressures in poorly conditioned tunnels and is highly susceptible to errors, due to leaks around the tunnel periphery because of badly sealed holes, access ports, etc. All of the preceding methods may require comparatively complicated data processing.

A simple method to estimate sectional lift would be of great value if it is easy to implement and use, requires minimal data processing, and does not require calibration. Frequently, tunnels are not equipped for force-balance mounting (or one is not available) and models are not amenable or designed for pressure tapping (e.g., smoke tunnels or when performing on-surface flow visualization). In this paper, a method to estimate sectional lift is described. The technique does not require calibration and employs only two pitot-static tubes in a specific geometric layout. The method development and experimental validation are presented.

Theoretical Development

In this technique, the two pitot-static tubes are inserted into the wind tunnel, as shown in Fig. 1. The static ports of the two pitot-static tubes are located in line with the airfoil profile's quarter-chord (with the presumption that this is the approximate location of the aerodynamic center). Variable definitions are shown in Fig. 1. In the development, it is assumed that the model is located at the tunnel centerline. Naturally, any point-velocity measurement device can be used at the two measurement locations (e.g., a hot wire anemometer, etc.). Such systems require calibration, however. Streamlines above the quarter-chord are approximately parallel to the freestream, whereas those below the wing usually have a slight downward inclination when positive lift is generated. Because pitot-static-tube accuracy only degrades for flow angularities greater than $\pm 15^\circ$ [1], streamline inclination is unlikely to cause error unless the pitot-static tubes are located excessively close to the wing, which will most likely violate the validity of Eq. (1).

The velocity measured by either pitot-static tube will contain components of the freestream and those induced by the presence of the wing. It is assumed that the wing may be modeled as a bound 2-D vortex located at the quarter-chord. In the following development, the absolute value of distances h and H are used, and the velocity direction is accounted for in the equations by setting the signs of the terms. This approach is adopted because, in most instances, distances of the pitot-static tube and the wing will be measured from the upper and lower tunnel walls. Consequently, their absolute value is determined. The velocity induced by this vortex is [3]

$$w_v = \frac{\Gamma}{2\pi h} \quad (1)$$

where h is the magnitude of the distance from the vortex to the point of interest.

[†]Data available online at http://www.iag.uni-stuttgart.de/laminarwindkanal/measurement_technique.htm [retrieved 6 December 2007].

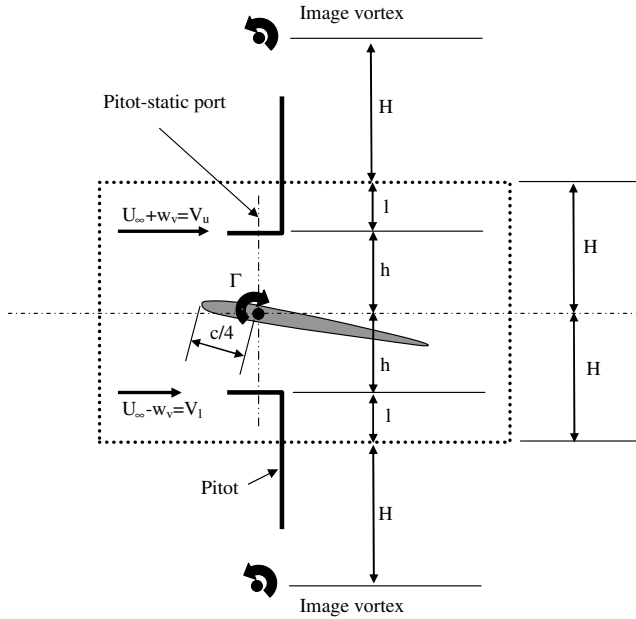


Fig. 1 Wing and image system geometry and nomenclature; two image vortices are shown.

The velocity difference between the upper and lower pitot-static tubes may be expressed as

$$V_u - V_l = U_\infty + w_v - (U_\infty - w_v) \quad (2)$$

which, upon substitution of Eq. (1), gives

$$V_u - V_l = \frac{\Gamma}{2\pi h} + \frac{\Gamma}{2\pi h} \quad (3)$$

Isolating for Γ , the wing's circulation yields

$$\Gamma = \pi h(V_u - V_l) \quad (4)$$

However, for practical wind-tunnel applications, V_u and V_l also contain induced velocities due to the presence of the wind-tunnel walls. These wall effects must be removed (the corrected velocities will be denoted by an overbar). Consequently, Eq. (4) can be written as

$$\Gamma = \pi h(\bar{V}_u - \bar{V}_l) \quad (5)$$

The presence of the upper and lower walls will be simulated by suitably positioned image vortices of equal strength to the wing's bound vortex. A similar configuration is used when modeling streamline curvature. In the development, four image vortices (two above and two below) will be used, allowing the determination of the infinite vortex series sequence. The layout of the first set of image vortices is shown in Fig. 1. Velocity measured by the upper (and lower) pitot-static tube will contain components due to the presence of the tunnel walls. These components must be removed (hence, their sign in the following equations is opposite to the direction of the velocity that the image vortices induce). With this correction, the velocity may be written as

$$\bar{V}_u = V_u - \frac{\Gamma}{2\pi(H+l)} + \frac{\Gamma}{2\pi(2H+l)} + \frac{\Gamma}{2\pi(2H+h)} - \frac{\Gamma}{2\pi(3H+h)} \quad (6)$$

where the second and third terms on the right-hand side are the upper-image-vortex contribution, and the fourth and fifth terms are the lower-image-vortex contribution. For the lower pitot-static tube,

$$\bar{V}_l = V_l + \frac{\Gamma}{2\pi(H+l)} - \frac{\Gamma}{2\pi(2H+l)} - \frac{\Gamma}{2\pi(2H+h)} + \frac{\Gamma}{2\pi(3H+h)} \quad (7)$$

Substitution of Eqs. (6) and (7) into Eq. (5) yields

$$\Gamma = \pi h \left(V_u - \frac{\Gamma}{2\pi(H+l)} + \frac{\Gamma}{2\pi(2H+l)} + \frac{\Gamma}{2\pi(2H+h)} - \frac{\Gamma}{2\pi(3H+h)} - \left[V_l + \frac{\Gamma}{2\pi(H+l)} - \frac{\Gamma}{2\pi(2H+l)} - \frac{\Gamma}{2\pi(2H+h)} + \frac{\Gamma}{2\pi(3H+h)} \right] \right) \quad (8)$$

Solving Eq. (8) for the circulation yields

$$\Gamma = \pi(V_u - V_l) / \left(\frac{1}{h} + \frac{1}{(H+l)} - \frac{1}{(2H+l)} - \frac{1}{(2H+h)} + \frac{1}{(3H+h)} \right) \quad (9)$$

By the Kutta–Joukowski theorem, the circulatory lift per unit span associated with the flow over a bound vortex is given by

$$l = \rho U_\infty \Gamma = \frac{1}{2} \rho U_\infty^2 c C_l \quad (10)$$

Thus, the sectional lift coefficient expressed in terms of circulation may be written as

$$C_l = \frac{2\Gamma}{U_\infty c} \quad (11)$$

Substitution of Eq. (9) into Eq. (11) yields an expression to estimate the lift coefficient of a profile based upon measurement of the differential velocity at designated locations above and below the airfoil's quarter-chord, with correction for wall effects using four image vortices. Substitution of $l = H - h$ yields

$$C_l = \frac{2\pi(V_u - V_l)}{U_\infty c} / \left(\frac{1}{h} + \frac{1}{(2H-h)} - \frac{1}{(3H-h)} - \frac{1}{(2H+h)} + \frac{1}{(3H+h)} \right) \quad (12)$$

Manipulation of the denominator of Eq. (12) results in

$$C_l = \frac{2\pi(V_u - V_l)}{U_\infty c} / \left(\frac{1}{h} + 2h \left[\frac{1}{4H^2 - h^2} - \frac{1}{9H^2 - h^2} \right] \right) \quad (13)$$

The denominator terms in square brackets are identified as the initial terms of an alternating series, where the H^2 term has coefficients of 4 and 9 and for additional image vortices, 16 and 25, etc. Expressing this as a series gives

$$C_l = \frac{2\pi(V_u - V_l)}{U_\infty c} / \left(\frac{1}{h} + 2h \left[\sum_{i=2}^{\infty} \frac{(-1)^i}{i^2 H^2 - h^2} \right] \right) \quad (14)$$

Summing this series to infinity yields

$$C_l = \frac{2\pi(V_u - V_l)}{U_\infty c} / \left(\frac{1}{h} + \frac{2ha}{bH^2 - h^2} \right) \quad (15)$$

where $a = 0.604681$ and $b = 3.405466$.

For comparison purposes, a solution using only two image vortices is given by

$$C_l = \frac{2\pi(V_u - V_l)}{U_\infty c} / \left(\frac{1}{h} + \left[\frac{2h}{4H^2 - h^2} \right] \right) \quad (16)$$

For some experimental setups, it may be useful to estimate C_l if the wing is displaced vertically. An infinite-image-vortex solution,

allowing the wing to be offset from the tunnel centerline, did not yield a compact expression in the spirit of the analysis; however, using only two image vortices (one above and one below) gives

$$C_l = \frac{4\pi(V_u - V_l)}{U_\infty c} \left/ \left(\frac{1}{h_u} + \frac{1}{h_l} - \left(\frac{1}{(2H_l + h_u)} + \frac{1}{(2H_u + h_l)} - \frac{1}{(H_l + l)} - \frac{1}{(H_u + l)} \right) \right) \right. \quad (17)$$

Numerical evaluation of Eq. (17) indicated that the small vertical movement of the quarter-chord that may occur for models that are mounted such that they rotate around their midchord (i.e., if a wall plug is used) has a negligible effect on the estimated C_l . Note that for even greater simplicity, the method may function with only one pitot-static tube mounted either above or below the wing. In this instance, the $V_u - V_l$ term in Eqs. (15) and (17) is replaced by $2(V_u - U_\infty)$ if the upper pitot-static tube is used.

Predictions of Eqs. (15) and (16) were evaluated experimentally using estimates of the lift coefficient obtained by surface-pressure integration. Tests were undertaken in Embry-Riddle's low-speed 1 by 1 ft open-return wind tunnel. A S8036 profiled wing was designed and rapid-prototyped. The wing spanned the tunnel. The model contained pressure taps in different layouts and was originally designed to evaluate the accuracy of different tapping layouts at low Reynolds numbers. Tappings inclined at 30 deg were used in this study because they have been shown to not trip the boundary layer. The chordwise pressure distribution was then integrated to yield the lift coefficient. The tests were run at 30 m/s, yielding a Reynolds number of 170,000. Additional experimental details of the wing and setup may be found in [2].

Pressure measurement was facilitated using an electronic pressure scanner that was designed and manufactured in-house. The scanner consists of 30 independent temperature-compensated differential pressure transducers. The transducers are connected through solenoid valves to the measurement ports. A custom interface was written in Visual Basic to control the valves as well as process and record the measured pressures. The valves were used to facilitate automatic zeroing of the transducers while running, eliminating any null or thermal offset effects. The pressure-transducer outputs were digitized using a 32-channel 16-bit National Instruments external USB analog-to-digital converter board. The board allows scanning of the pressures at up to 250,000 readings per second. All processed pressures are the average of 1000 readings. Calibration of the scanner was performed using a FlowKinetics FKT 1-DP1A-SV pressure/flow meter. The FKT meter is calibrated against a deadweight primary standard and was within its calibration specifications. Comparison with the standard showed accuracy of better than 0.5 Pa.

Calibration and comparison of the scanner with the FKT meter showed measured pressure agreement within 0.8 Pa for all 30 of the transducers. The uncertainty interval for the pressure coefficient C_p was estimated using the method of Kline and McClintock [4]. The uncertainty was estimated as $w_{C_p}/C_p = 0.2\%$. Velocities from the two pitot-static tubes located above and below the wing, as well as that monitoring the freestream, were recorded using a FlowKinetics LLC FKT 3-DP1A meter. This instrument measures atmospheric pressure and relative humidity and uses these measurements to calculate air density for velocity calculations. The meter also contains three independent differential pressure transducers that were used to measure the pressures indicated by the pitot-static tubes (two for lift measurement and one for the tunnel freestream). Comparison with a primary standard indicated accuracy better than 0.1% for all three transducers.

Before the tests were undertaken, the jet was surveyed at the pitot-static-tube locations without the wing present. This was to establish any velocity nonuniformity that otherwise may be attributed to lift generation. Evaluation of the method is presented in Figs. 2 and 3. Figure 2 presents the measured velocity difference between the upper and lower pitot-static tubes for vertical pitot-static-tube locations of 3, 4, and 5 in. from the airfoil's quarter-chord. The results show that the differential velocity is in fact quite large and is well within the resolution of most research-grade manometers. The differential velocity decreases as the pitot-static tubes are positioned closer to the walls. Also shown on the plot is the average of the upper and lower velocities; $(V_u + V_l)/2$ divided by the measured freestream velocity. The data indicate that the average velocity is generally within 1% of the measured U_∞ value. Thus, for even greater simplicity, it may be possible to implement the method with only two pitot-static tubes (i.e., no additional pitot-static tube to measure the freestream), using both their difference (lift estimate) and average values (freestream estimate). What is also implied is that using a single pitot-static tube to measure the freestream velocity in a wind tunnel can cause erroneous values if badly placed; two symmetrically located pitot-static tubes would be more reliable and would negate airfoil/wing lifting effects if a system using tappings on the contraction and test section is not available.

Figure 3a presents lift-coefficient estimates excluding wall effects: that is, setting $H = \infty$ in Eq. (15). C_l is systematically overestimated, compared with the pressure-integration data, which is regarded as the reference value for the airfoil section in these tests. Decreasing pitot-static-tube proximity to the walls increases the estimated C_l . Accounting for the upper and lower walls using two image vortices shows the three data series collapsing onto the pressure-integration result (see Fig. 3b). Figure 3c shows the estimated lift coefficient when using an infinite series of image vortices to approximate the walls. As may be seen, the plot is slightly

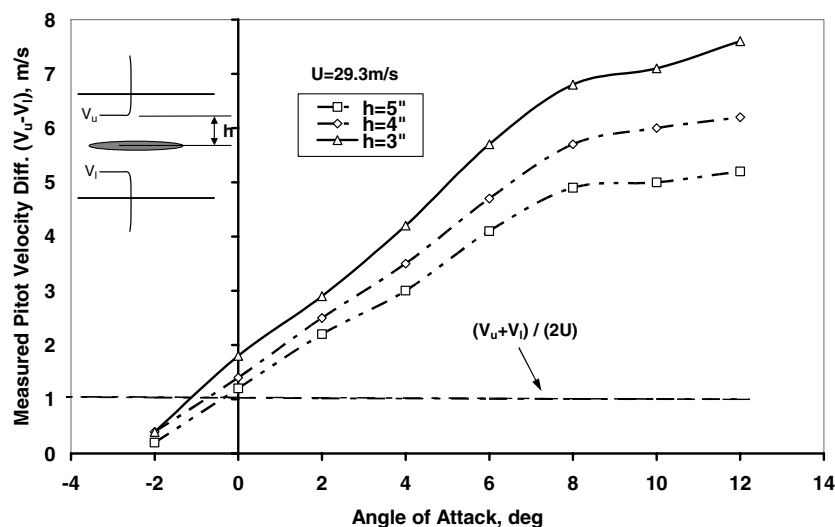
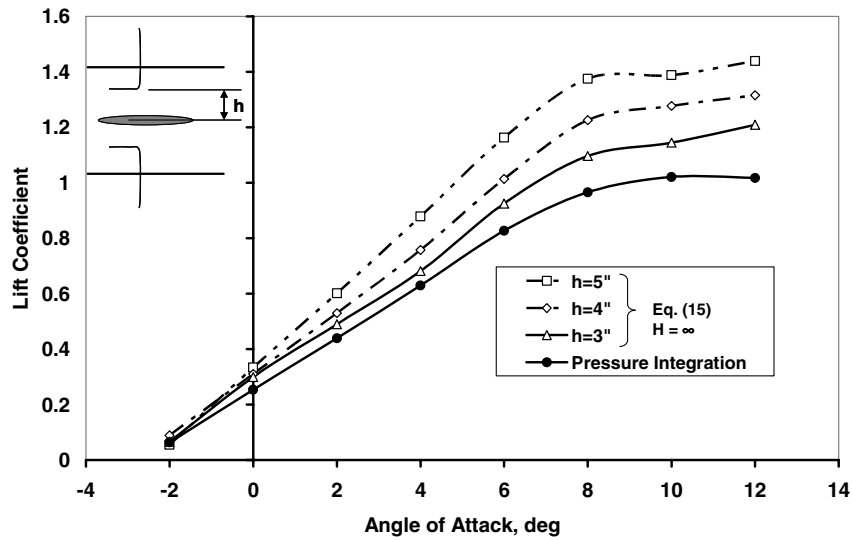
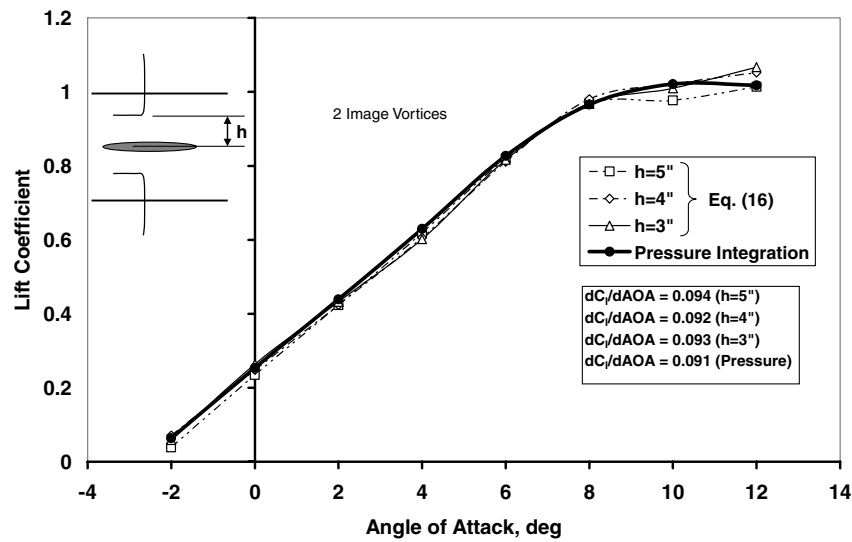


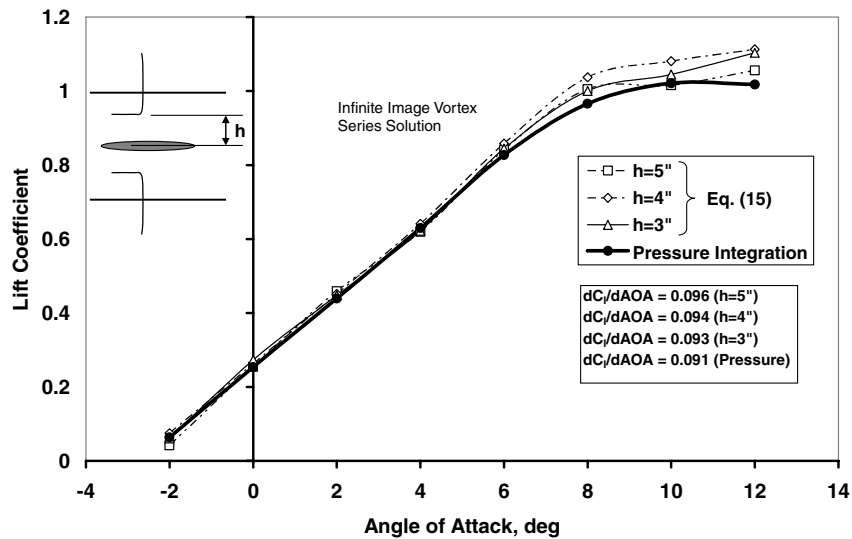
Fig. 2 Measured velocity differential between the upper and lower pitot-static tubes.



a)



b)



c)

Fig. 3 Calculated lift coefficient a) excluding wall effects, b) including wall effects (two image vortices), and c) including wall effects (∞ image vortices); AOA denotes the angle of attack.

rotated, yielding C_l estimates marginally higher than the two-image-vortex approximation (Fig. 3b). The infinite series yields a better estimate in the linear region than the two-term approximation, but it overpredicts in the stall regime. The agreement in the stall regime of Eq. (16) may be fortuitous. An overprediction of lift is likely because the separated flow region over the suction side would most likely lead to an increase in measured velocity between the upper surface and tunnel wall (analogous in concept to wake blockage). The data suggest that for the present experimental setup (i.e., $c/2H = 1/3$), the two-image-vortex solution shows close accord with the infinite-image-vortex solution. Consequently, Eq. (17) may be used for models that are displaced off the tunnel centerline.

Considering the simplicity of the present method, the agreement with the pressure-integration data is excellent. Generally, reasonably close wing–pitot-static-tube proximity ($h/c \approx 0.75 \rightarrow 1$) may be preferable to maximize the velocity differential if the accuracy or resolution of the differential pressure measurement system is marginal. If required, drag data can be acquired using a rake wake [1]. Consequently, a pressure scanner could be used to read the pitot-static tubes for lift and the rake wake for drag to yield composite lift and drag data.

Conclusions

A method to measure the lift coefficient of an airfoil is presented that requires only the use of two pitot-static tubes or point-velocity measurement devices. The technique could easily be implemented in facilities in which lift estimation is not physically or financially viable to implement using more traditional means. In the method, the

pitot-static ports are positioned above and below the airfoil's quarter-chord. The velocity difference between the two tubes is used, via the Kutta–Joukowski theorem, to estimate the sectional lift coefficient. The presence of the upper and lower walls is accounted for using an image system. Comparison with experimental data show excellent agreement between the method and C_l estimated by surface-pressure integration.

Acknowledgments

The author would like to thank the Associate Editor and the reviewer for their helpful comments and suggestions. The author would also like to thank Dan Michalek, Alicia Ziegler, Bart Brown, Francis Phan and James Kooiman for performing the wind-tunnel tests.

References

- [1] Rae, W., and Pope, A., *Low-Speed Wind Tunnel Testing*, Wiley, New York, 1984, pp. 344–401.
- [2] Traub, L. W., and Cooper, E., “Experimental Investigation of Pressure Measurement and Airfoil Characteristics at Low Reynolds Numbers,” *Journal of Aircraft*, Vol. 45, No. 4, 2008, pp. 1322–1333. doi:10.2514/1.34769
- [3] Houghton, E. L., and Carpenter, P. W., *Aerodynamics for Engineering Students*, Butterworth Heinemann, Oxford, England, 2003, pp. 113–135.
- [4] Kline, S. J., and McClintock, F. A., “Describing Uncertainties in Single Sample Experiments,” *Mechanical Engineering*, Vol. 75, Jan. 1953, pp. 3–8.